

<https://helda.helsinki.fi>

Effect of Mn and Mg dopants on vacancy defect formation in ammonothermal GaN

Heikkinen, T.

2020-10-01

Heikkinen, T., Pavlov, J., Ceponis, T., Gaubas, E., Zajac, M. & Tuomisto, F. 2020, 'Effect of Mn and Mg dopants on vacancy defect formation in ammonothermal GaN', Journal of Crystal Growth, vol. 547, 125803. <https://doi.org/10.1016/j.jcrysgr.2020.125803>

<http://hdl.handle.net/10138/346137>

<https://doi.org/10.1016/j.jcrysgr.2020.125803>

cc_by_nc_nd

acceptedVersion

Downloaded from Helda, University of Helsinki institutional repository.

This is an electronic reprint of the original article.

This reprint may differ from the original in pagination and typographic detail.

Please cite the original version.

Effect of Mn and Mg dopants on vacancy defect formation in ammonothermal GaN

T. Heikkinen^{1,2}, J. Pavlov³, T. Ceponis³, E. Gaubas³, M. Zając⁴, F. Tuomisto^{1,2}

¹Department of Physics and Helsinki Institute of Physics, University of Helsinki, 00014
Helsinki, Finland

²Department of Applied Physics, Aalto University, 00076 Aalto Espoo, Finland

³Institute of Photonics and Nanotechnology, Vilnius University, Saulėtekio 3, 10257 Vilnius,
Lithuania

⁴Institute of High Pressure Physics, Polish Academy of Sciences, Sokołowska 29/37, 01-142
Warsaw, Poland

Abstract

We have applied positron annihilation spectroscopy to study the formation of Ga vacancy related defects in Mg and Mn doped bulk GaN crystals grown by the ammonothermal method. We show that Mn doping has little or no effect on the formation of Ga vacancies, while Mg doping strongly suppresses their formation, in spite of both dopants leading to highly resistive material. We suggest the differences are primarily due to the hydrogen-dopant interactions. Further investigations are called for to draw a detailed picture of the atomic scale phenomena in the synthesis of ammonothermal GaN.

Introduction

The semiconductor material family of the III-nitrides, with its active wavelengths ranging from infrared to ultraviolet, has a wide range of applications in optoelectronics. To make full use of their potential, high quality lattice-matched substrates are crucial. Extended defects in the substrate can penetrate into the overgrown layers and have a considerable impact on the device characteristics. As a consequence, they have been studied extensively in order to find optimal growth conditions to minimize their density. While point defects mostly influence the electrical and optical characteristics of the substrate itself, with less impact on the properties of the overgrown structures, they can have a significant role in the formation of the extended defects, such as inversion layers and dislocations. For the past two decades the need of better quality substrates has driven the development of nitride growth techniques capable of producing either true bulk crystals [1-6], several millimeters thick hetero-epitaxial layers to be separated from foreign substrates (see, e.g., [7, 8] for a review), or a combination of these approaches [9, 10]. Originally growing bulk GaN substrates with very low dislocation densities (of the order $\sim 10^2$ cm^{-2}) was only possible by methods employing high temperatures and pressures ($\sim 1500^\circ\text{C}$, ~ 15 kbar) [1]. Currently, for example ammonothermal synthesis provides a way to grow material of similar or even better structural quality at much less extreme conditions ($\sim 500^\circ\text{C}$, ~ 3 kbar) [2-6]. However, the point defect distribution in ammonothermally grown GaN is quite different due to the much lower growth temperature, and strongly affected by growth kinetics and chemistry as well [11, 12]. A detailed understanding of the formation mechanisms of point defects is necessary for developing approaches that could minimize the unwanted effects they have on the material quality.

Positron annihilation spectroscopy is an effective and non-destructive method for investigating vacancy type defects in semiconductors. It has been widely applied to III-nitrides. Before

annihilating, positrons implanted into a sample can get trapped in and localize at neutral and negative vacancies due to their missing positive ion core. In practice the trapping causes well-defined changes in the positron–electron annihilation radiation, namely, an increase in the positron lifetime and a narrowing of the momentum distribution of the annihilating positron–electron pair (Doppler broadening) [13]. The annihilation data can be used to determine the vacancy concentration as well as to distinguish between different types of vacancies and their chemical environment. Performing measurements as a function of temperature provides additional information on the charge states of the detected defects. Introducing additional point defects by, e.g., particle irradiation allows to highlight differences in the original defect distributions when the latter are characterized by high concentrations producing only small apparent differences in the positron annihilation data.

In this work, we employ positron annihilation spectroscopy to investigate the effects of Mg and Mn doping on point defect formation in ammonothermally (AT) grown bulk GaN crystals. Introduction of both impurities at the $10^{18} - 10^{19} \text{ cm}^{-3}$ concentration level leads to highly resistive material (above $10^8 \text{ } \Omega\text{-cm}$ at room temperature), but with different optical properties [14-17]. In particular, luminescence experiments show that Mn doping leads to material with significantly higher concentrations of non-radiative recombination centers. We show that after the regular processing steps of the substrates, the most important being post-growth thermal treatment at 1100°C , both Mn and Mg acceptors are in the negative charge state (that is, they are ionized). However, both the nature and concentrations of the vacancy type defects differ significantly: the concentration of Ga vacancy related defects is more than an order of magnitude higher in Mn doped material, and in contrast to Mg doped materials, these vacancies are complexed with multiple hydrogen atoms.

Experimental details

The ammonothermally grown bulk GaN crystal samples were doped with either Mn ($1 \times 10^{19} \text{ cm}^{-3}$) or Mg ($1 \times 10^{18} \text{ cm}^{-3}$). The residual O and H concentrations in the samples are on the level of low- and mid- 10^{18} cm^{-3} , respectively [18]. After synthesis at 500°C the samples were annealed in N_2 atmosphere at 1100°C . For both sample series (Mn and Mg doped), we measured a pair of samples after this standard post-growth processing, as well as samples irradiated with 1-MeV neutrons [14] to fluences $1 \times 10^{16} \text{ cm}^{-2}$ and $5 \times 10^{16} \text{ cm}^{-2}$.

In this work, the positron lifetime was measured with a digital spectrometer with a timing resolution of 250 ps. A ~ 1 MBq positron source (^{22}Na encapsulated in $1.5 \mu\text{m}$ Al-foil) was sandwiched between two sample pieces. When measuring identical (un-irradiated) samples 1×10^6 annihilation events were collected in each spectrum. In order to have sufficient data when measuring the irradiated samples against a well-characterized GaN reference sample only producing annihilations in the lattice [11], 2×10^6 events were collected in each spectrum. We performed measurements in the temperature range 40 – 600 K using a closed-cycle He cryostat with resistive heating and high-temperature interface.

The positron lifetime spectra $n(t) = \sum_i I_i \exp(-t/\tau_i)$ were analyzed as the sum of exponential decay components convoluted with the resolution function of the spectrometer (a Gaussian), for details see, e.g., Ref. 13. The constant background, annihilations in the source material (together a few percent) and, when necessary, annihilations in the GaN reference side of the sandwich (50% of the counts after the source correction) were subtracted. A positron in state i (whether that is delocalized state in the lattice or localized state at a defect) annihilates with a lifetime τ_i and intensity I_i . An increase in the average positron lifetime ($\tau_{ave} = \sum_i I_i \tau_i$) above the bulk lattice lifetime τ_B (160 ps for GaN) indicates the presence of vacancy type defects in the material. As the center of mass of the spectrum τ_{ave} is insensitive to the decomposition

procedure, it is robust enough of a parameter that as small a change in its value as 1 ps can be reliably detected. To reliably decompose the spectrum to lifetime components, they must be sufficiently different from each other, at least by a factor 1.3 – 1.5. Typically only two lifetime components can be reliably separated from the spectrum measured from semiconductors (shorter τ_1 related to bulk and possibly defects with so short a lifetime that it cannot be separated, and τ_2 related to large enough defect(s) to produce high enough lifetime to be separated).

The temperature dependent kinetic trapping model (described, e.g., in Ref. 13) can be used to analyze the temperature behavior of τ_{ave} . The trapping coefficient to a neutral vacancy (μ_V) is temperature independent while the trapping coefficient to a negative vacancy (μ_{V^-}) varies as $T^{0.5}$. For vacancies with concentration c_V the positron trapping rate is $\kappa_V = \mu_V c_V$ (with $\mu_V = 3 \times 10^{15} \text{ s}^{-1}$ for negatively charged Ga vacancies in GaN at 300 K). In addition to vacancies, negative ions can also trap positrons at hydrogen-like Rydberg states at low temperatures. The positron trapping coefficient to these shallow traps (μ_{st}) also varies as $T^{0.5}$. Unlike vacancy type defects, shallow traps allow positrons to escape the trap at elevated temperatures due to their low binding energy. The escape rate depends on the temperature and binding energy as $\delta_{st} = \mu_{st} (2\pi m^* k_B T / h^2)^{3/2} \exp(-E_{b,st} / k_B T)$.

Results

Figure 1 shows the average positron lifetime (τ_{ave}) at temperatures ranging from 40 to 600 K in the Mn and Mg doped samples before irradiation. All the measured values are higher than those measured in the reference sample that gives the bulk positron lifetime in GaN ($\tau_B \approx 160 \text{ ps}$) [11]. This clearly indicates presence of vacancy type defects in the un-irradiated samples. Decomposing the spectra into lifetime components was not possible, which indicates either

saturation trapping of positrons (high vacancy defect concentrations) or the presence of more than one vacancy type defect efficiently trapping positrons, leading to several different lifetime components making the fitting procedures fail. The temperature behavior of τ_{ave} in the Mg doped AT GaN resembles previous results obtained in nominally undoped high-nitrogen-pressure (HNP) GaN [11, 19-21], where the O concentration is high, in the mid- 10^{19} cm^{-3} range, and the Mg concentration is of the order of 10^{18} cm^{-3} . In contrast, the temperature behavior of τ_{ave} in the Mn doped AT GaN resembles that of nominally undoped AT GaN [22] with O and Mg contents an order of magnitude lower than those in HNP GaN, but where the H concentrations are also significant, in the mid- 10^{18} cm^{-3} range. The average lifetime is relatively close to τ_B at low temperatures in both the Mn and Mg doped samples, increases strongly at 200 – 350 K, and appears to saturate above 350 K. This behavior is typical of negative ions (shallow traps for positons) competing with vacancies in positron trapping at low temperatures. The main differences between the two types of samples are: (1) the average lifetime is roughly 5 ps longer in the Mn doped sample throughout the temperature range of the experiment, and (2) at high temperatures τ_{ave} increases with temperature in the Mn doped sample while it decreases in the Mg doped sample.

The average positron lifetime obtained in the 1-MeV neutron irradiated Mg and Mn doped samples are presented in Figs. 2 and 3, respectively. Both figures show data from samples irradiated to fluences 1×10^{16} cm^{-2} and 5×10^{16} cm^{-2} , as well as data from the unirradiated and reference samples for comparison. The experiments on irradiated samples were carried out below room temperature (40-300 K) in order to avoid thermal recovery [23]. The average lifetime increases in the Mg doped samples (Fig. 2) a little after the 1×10^{16} cm^{-2} irradiation and significantly after the 5×10^{16} cm^{-2} irradiation. In both cases, the increase is roughly constant throughout the temperature range, suggesting that only vacancy defects are introduced at significant concentrations in the irradiation. Separating lifetime components was not possible

in the Mg doped samples after irradiation either, indicating that vacancies introduced in the irradiation are monovacancy-sized instead of larger vacancy clusters or voids. The fact that the irradiation-induced introduction of vacancy defects is clearly visible in τ_{ave} , allows us to conclude that positron trapping is not at saturation in the Mg doped AT GaN samples prior to irradiation. In contrast to the Mg doped samples, the average positron lifetime shows no change after the 1-MeV neutron irradiation with either fluence (Fig. 3), except for a barely observable increase at low temperatures after the $5 \times 10^{16} \text{ cm}^{-2}$ irradiation. This in turn implies that the trapping of positrons is in saturation in the unirradiated Mn doped AT GaN samples, making the defects introduced in the irradiation have little effect on the defect distribution detected with positrons.

Discussion

The increase of the average positron lifetime in the irradiated Mg doped samples shows that positron trapping cannot be at saturation in the unirradiated samples. This allows us to estimate defect concentrations by fitting the kinetic trapping model [13] to the experimental data. The fitted curve shown in Fig. 1 corresponds to a concentration of $[V_{Ga}] = 9 \times 10^{16} \text{ cm}^{-3}$ for Ga vacancies in the negative charge state (with a vacancy lifetime of $\tau_D = 235 \text{ ps}$), and a negative ion concentration of $c_{ion} = 2 \times 10^{18} \text{ cm}^{-3}$. The fitted negative ion concentration agrees well with the Mg doping concentration of $1 \times 10^{18} \text{ cm}^{-3}$, suggesting that all the Mg dopants are ionized as acceptors in these samples and are the dominant shallow trap for positrons, similarly as in HNP GaN [19].

The kinetic trapping model can be fitted to the data obtained in the irradiated samples as well (curves in Fig. 2). However, the results are less accurate compared to the unirradiated samples, due to more scatter in the experimental data and to the limited temperature range. In spite of

these limitations, it appears that any increase in the concentration of negative ion type defects possibly introduced in the irradiation is small compared to the original concentration of $c_{\text{ion}} = 2 \times 10^{18} \text{ cm}^{-3}$. The fitted curves in Fig. 2 correspond to negative Ga vacancy concentrations of $1.2 \times 10^{17} \text{ cm}^{-3}$ and $3 \times 10^{17} \text{ cm}^{-3}$ for the $1 \times 10^{16} \text{ cm}^{-2}$ and $5 \times 10^{16} \text{ cm}^{-2}$ irradiated samples, respectively, with no change in the negative ion concentrations. These values translate to concentrations of irradiation-induced Ga vacancies of $3 \times 10^{16} \text{ cm}^{-3}$ and $2 \times 10^{17} \text{ cm}^{-3}$ in the two irradiations, or an introduction rate for 1-MeV neutron irradiation of about $\Sigma = 3 - 4 \text{ cm}^{-1}$. In 2-MeV electron irradiation experiments [23] it was found that the introduction rate of negative ions was four-fold compared to that of Ga vacancies. If a comparable relation holds in the neutron irradiation performed in this work, this would suggest that the concentration of negative ions introduced in the irradiation would be at most half of the original negative ion concentration even after the higher fluence, in line with our observations.

The irradiation appears to introduce very little new defects compared to the original concentrations in the Mn doped samples, as hardly any change in τ_{ave} is visible between the samples in Fig. 3. It is likely that the neutron irradiation introduces defects in the same way in both Mg and Mn doped samples, implying that the original concentrations of the vacancy defects and negative ions in the Mn doped samples need to be an order of magnitude higher than those introduced in the irradiation, i.e., at least in the mid- 10^{18} cm^{-3} range. This is in line with the very similar experimental data obtained in nominally undoped AT GaN [22], where we interpreted the results as Ga vacancy-multihydrogen complexes (with $\tau_D = 185 \text{ ps}$) at concentrations above $5 \times 10^{18} \text{ cm}^{-3}$. The abrupt change in the temperature behavior at around 300 K suggests that these vacancy complexes are in the neutral (instead of negative) charge state.

Assuming a negative ion concentration of $1 \times 10^{19} \text{ cm}^{-3}$ (matching the Mn concentration) allows us to fit the average lifetime with $1.5 \times 10^{19} \text{ cm}^{-3}$ of neutral vacancy complexes with a

defect lifetime of $\tau_D = 185$ ps in the Mn doped samples as shown with the curve in Fig. 1. This is well in line with the saturation trapping discussed above. Adding a third type of defect at concentrations likely introduced in the irradiation (negative Ga vacancy, $\tau_D \approx 235$ ps) to the kinetic trapping model increases the average lifetime by at most 1 ps at low temperatures, comparable to the experimental difference after the highest fluence irradiation (Fig. 3). These observations strongly support the interpretation that positron trapping is saturated at reduced-open volume Ga vacancy related defects, likely Ga vacancy-multihydrogen complexes, in Mn doped AT GaN. The slight rise in τ_{ave} at the highest temperatures in the unirradiated Mn doped samples is also similar to that observed earlier in undoped AT GaN samples [22], suggesting the presence Ga vacancy defects with different amounts of complexed hydrogen.

In spite of both Mg and Mn doping of AT GaN leading to highly resistive material after post-growth annealing at 1100°C, the effects of the two dopants on the formation of other acceptor-type defects, namely Ga vacancies, are dramatically different. The Ga vacancy concentration in Mg doped samples is two orders of magnitude lower than that in the Mn doped samples (less than 10^{17} cm⁻³ compared to more than 1×10^{19} cm⁻³), although the acceptor-type dopant concentrations are an order of magnitude higher in the Mn-doped samples, implying that Fermi level effects and thermal formation of vacancies are not significant in determining the defect concentrations. In addition, in Mn doped AT GaN the Ga vacancies appear very efficiently hydrogenated while in Mg doped AT GaN there is no evidence of significant hydrogen involvement in the Ga vacancy defects. In fact, Mn doping appears to have no effect whatsoever on the Ga vacancy formation as the data are essentially the same as in undoped AT GaN samples [22]. Interestingly, the effect of Mg doping appears to have a particularly strong effect on the atomic level structure of AT GaN. It is worth noting that typically in AT GaN the point defect concentrations are much higher than can be predicted taking into account only thermal formation [11, 22, 24], interpreted as the growth (surface) kinetics and chemistry

dominating the formation mechanisms. In the present Mg doped AT GaN, annealed at 1100°C, the point defect distribution is essentially the same as in HNP GaN that is grown in conditions much closer to thermal equilibrium, implying that the addition of Mg in the GaN lattice limits the kinetically-driven Ga vacancy-multihydrogen complex formation during growth of AT GaN. This is in agreement also with the results obtained in Mg doped AT GaN before post-growth annealing [11], where no defects were observed with positrons.

The significant difference between the migration properties of Mg and Mn, with Mg having a significantly higher activation energy of diffusion than Mn [25, 26], suggests that the kinetic effects should be even stronger with Mg than with Mn, opposite to what we observe. A possible mechanism could be the strong affinity of hydrogen to the Mg impurities, which could lead to dehydrogenation of the Ga vacancies, allowing them to migrate during growth (at around 550°C), as “clean” Ga vacancies are mobile already at 300°C [23]. This could lead to the Ga vacancy concentration stabilizing as defined by thermal formation at the growth temperature, i.e., very low, explaining their non-observation directly after growth [11]. The emergence of Ga vacancies after the post-growth annealing could be due to their thermal formation and subsequent stabilization by either O or H (as both are abundant in AT GaN), but through migration and pairing that rarely leads to complexes involving more than two defects [27-29]. Further investigations are clearly needed to create a detailed understanding of the microscopic mechanisms determining the atomic-scale structure of GaN grown by the ammonothermal method.

Summary

We have applied positron annihilation spectroscopy to study vacancy formation in Mg and Mn doped bulk GaN crystals grown by the ammonothermal method. By comparing temperature-

dependent data obtained in post-growth annealed samples and samples irradiated with neutrons to various fluences, we are able to highlight initially weakly observable differences in the differently doped materials. Mn doping has little or no effect on the formation of Ga vacancy related defects, while Mg doping strongly suppresses their formation, in spite of both dopants leading to semi-insulating material. We suggest the differences are primarily due to the hydrogen-dopant interactions, but further investigations are necessary to obtain a detailed understanding of the microscopic mechanisms dictating the atomic scale structure in ammonothermal synthesis of GaN.

Acknowledgments

This work was partially funded by Academy of Finland (Project Nr 315082).

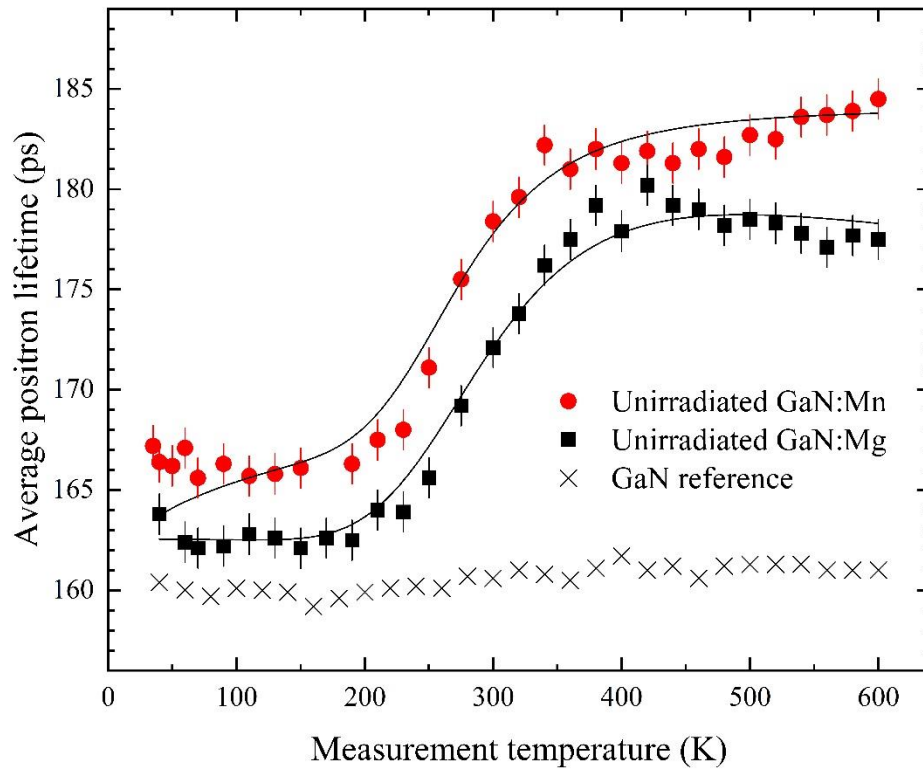


Fig. 1 The average positron lifetime measured as a function of temperature in unirradiated Mn and Mg doped bulk ammonothermal GaN, as well as defect free reference. The solid lines show the kinetic trapping model (with negative Ga vacancies and negative ions for GaN:Mg and neutral Ga vacancy-multihydrogen complexes and negative ions for GaN:Mn) fitted to the data. The error bars for the GaN reference data are smaller than the symbol size.

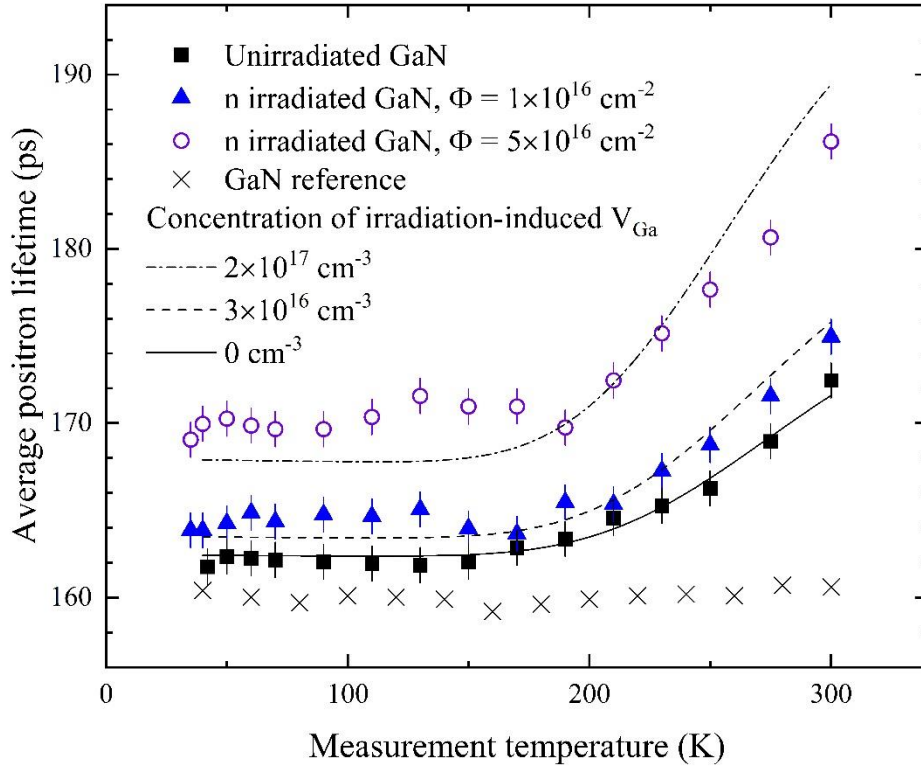


Fig. 2 The average positron lifetime measured as a function of temperature in Mg doped bulk ammonothermal GaN, as well as in a GaN reference. The solid and dashed lines show the kinetic trapping model (with negative Ga vacancies and negative ions) fitted to the data. The error bars for the GaN reference data are smaller than the symbol size.

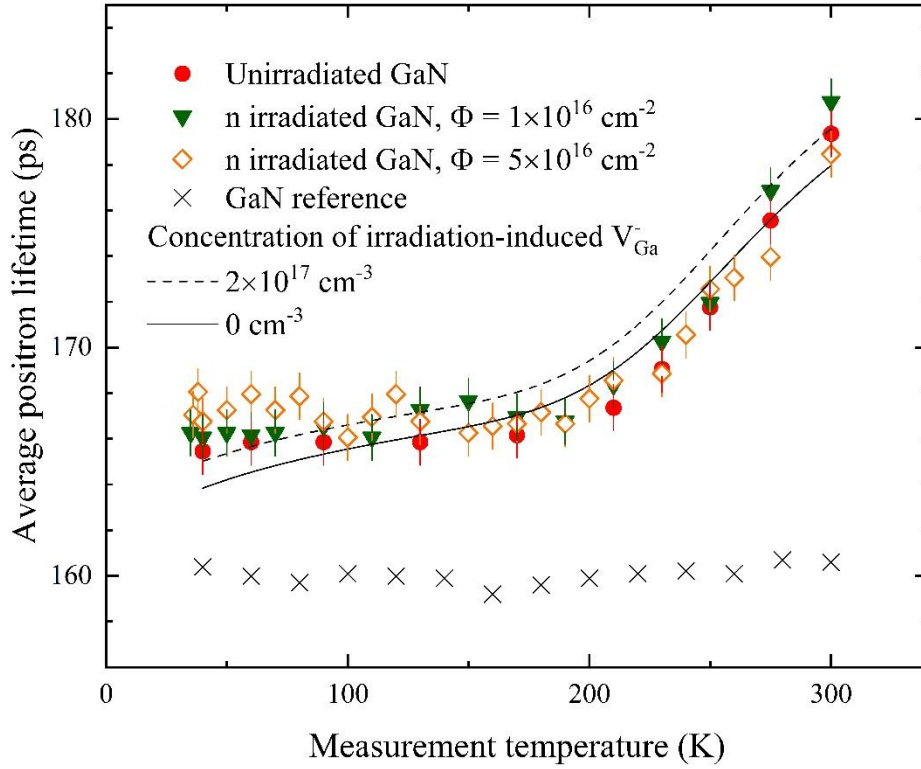


Fig. 3 The average positron lifetime measured as a function of temperature in Mn doped bulk ammonothermal GaN, as well as defect free reference. The solid and dashed lines represent the kinetic trapping model before and after adding third defect type (negative Ga vacancy in addition to neutral Ga vacancy-multihydrogen complexes and negative ions) in a concentration that increases the average positron lifetime the amount seen at low temperatures in the experimental data. The error bars for the GaN reference data are smaller than the symbol size.

References

- [1] I. Grzegory, S. Krukowski, M. Leszczynski, P. Perlin, T. Suski, S. Porowski, The Application of High Pressure in Physics and Technology of III-V Nitrides, *Acta Phys. Pol. A* **100 (Suppl)** (2001) 57
- [2] R. Dwiliński, R. Doradziński, J. Garczyński, L. P. Sierzputowski, A. Puchalski Y. Kanbara, K. Yagi, H. Minakuchi, H. Hayashi, Bulk ammonothermal GaN, *J. Cryst. Growth* **311** (2009) 3015
- [3] E. Letts, T. Hashimoto, I. Masanori, Y. Nojima, Development of GaN wafers for solid-state lighting via the ammonothermal method, *J. Cryst. Growth* **350** (2012) 66
- [4] Y. Mori, M. Imade, K. Murakami, H. Takazawa, H. Imayabashi, U. Todoroki, K. Kitamoto, M. Maruyama, M. Yoshimura, Y. Kitaoka, T. Sasaki, Growth of bulk GaN crystal by Na flux method under various conditions, *J. Cryst. Growth* **350** (2012) 72
- [5] S.Pimputkar, S. Kawabata, J. S. Speck, S. Nakamura, Surface morphology study of basic ammonothermal GaN grown on non-polar GaN seed crystals of varying surface orientations from m-plane to a-plane, *J. Cryst. Growth* **368** (2013) 67
- [6] D. Ehretraut, R. T. Pakalapati, D. S. Kamber, W. K. Jiang, D. W. Pocius, B. C. Downey, M. McLaurin, M. P. D'Evelyn, High Quality, Low Cost Ammonothermal Bulk GaN Substrates, *Jpn. J. Appl. Phys.* **52** (2013) 08JA01
- [7] H. Morkoç, Comprehensive characterization of hydride VPE grown GaN layers and templates, *Mater. Sci. Eng. Rep.* **33** (2001) 135
- [8] Y. Oshima, T. Yoshida, T. Eri, K. Watanabe, M. Shibata, T. Mishima, in: D. Ehretraut, E. Meissner, M Bockowski (Ed.), *Technology of Gallium Nitride Crystal Growth*, Springer, Berlin, 2010, p. 79
- [9] M. Bockowski, I. Grzegory, B. Łuczniak, T. Sochacki, G. Nowak, B. Sadovyi, P. Strąk, G. Kamler, E. Litwin-Staszewska, S. Porowski, Multi feed seed (MFS) high pressure crystallization of 1–2 in GaN, *J. Cryst. Growth* **350** (2012) 5
- [10] T. Sochacki, Z. Bryan, M. Amilusik, R. Collazo, B. Łuczniak, J.L. Weyher, G. Nowak, N. Sadovyi, G. Kamler, R. Kucharski, M. Zając, R. Doradziński, R. Dwiliński, I. Grzegory, M. Boćkowski, Z. Sitar, Preparation of Free-Standing GaN Substrates from Thick GaN Layers Crystallized by Hydride Vapor Phase Epitaxy on Ammonothermally Grown GaN Seeds *Appl. Phys. Express* **6** (2013) 075504
- [11] F. Tuomisto, J.-M. Mäki, M. Zając, Vacancy defects in bulk ammonothermal GaN crystals, *J. Cryst. Growth* **312** (2010) 2620
- [12] S. Suihkonen, S. Pimputkar, S. Sintonen, F. Tuomisto, Defects in Single Crystalline Ammonothermal Gallium Nitride, *Adv. Electron. Mater.* **3** (2017) 1600496
- [13] F. Tuomisto, I. Makkonen, Defect identification in semiconductors with positron annihilation: Experiment and theory, *Rev. Mod. Phys.* **85** (2013) 1583
- [14] J. Pavlov, T. Čeponis, L. Deveikis, T. Heikkinen, J. Raisanen, V. Rumbauskas, G. Tamulaitis, F. Tuomisto, E. Gaubas, Photoionization, photoluminescence and positron annihilation spectroscopy of defects in neutron-irradiated ammono-thermal GaN, *Lith. J. Phys.* **59** (2019) 179

- [15] M. A. Reshchikov, P. Ghimire, and D. O. Demchenko, Magnesium acceptor in gallium nitride. I. Photoluminescence from Mg-doped GaN, *Phys. Rev. B* **97** (2018) 205204
- [16] A. Wolos, A. Wyszomolek, M. Kaminska, A. Twardowski, M. Bockowski, I. Grzegory, S. Porowski, M. Potemski, Neutral Mn acceptor in bulk GaN in high magnetic fields, *Phys. Rev. B* **70** (2004) 245202
- [17] A. Wolos, M. Palczewska, M. Zajac, J. Gosk, M. Kaminska, A. Twardowski, M. Bockowski, I. Grzegory, S. Porowski, Optical and magnetic properties of Mn in bulk GaN, *Phys. Rev. B* **69** (2004) 115210
- [18] M. Zajac, R. Kucharski, K. Grabianska, A. Gwardys-Bak, A. Puchalski, D. Wasik, E. Litwin-Staszewska, R. Piotrkowski, J.Z Domagala, M. Bockowski, Basic ammonothermal growth of Gallium Nitride – State of the art, challenges, perspectives, *Prog. Cryst. Growth Charact. Mater.* **64** (2018) 63-74
- [19] K. Saarinen, T. Laine, S. Kuisma, J. Nissilä, P. Hautojärvi, L. Dobrzynski, J. M. Baranowski, K. Pakula, R. Stepniewski, M. Wojdak, A. Wyszomolek, T. Suski, M. Leszczynski, I. Grzegory, S. Porowski, Observation of Native Ga Vacancies in GaN by Positron Annihilation, *Phys. Rev. Lett.* **79** (1997) 3030
- [20] K. Saarinen, J. Nissilä, P. Hautojärvi, J. Likonen, T. Suski, I. Grzegory, B. Lucznik, S. Porowski, The influence of Mg doping on the formation of Ga vacancies and negative ions in GaN bulk crystals, *Appl. Phys. Lett.* **75** (1999) 2441
- [21] F. Tuomisto, K. Saarinen, B. Lucznik, I. Grzegory, H. Teisseyre, T. Suski S. Porowski, P. R. Hageman, J. Likonen, Effect of growth polarity on vacancy defect and impurity incorporation in dislocation-free GaN, *Appl. Phys. Lett.* **86** (2005) 031915
- [22] F. Tuomisto, T. Kuittinen, M. Zajac, R. Doradziński, D. Wasik, Vacancy–hydrogen complexes in ammonothermal GaN, *J. Cryst. Growth* **403** (2014) 114
- [23] F. Tuomisto, V. Ranki, D. C. Look, G. C. Farlow, Introduction and recovery of Ga and N sublattice defects in electron-irradiated GaN, *Phys. Rev. B* **76** (2007) 165207
- [24] F. Tuomisto, J.-M. Mäki, C. Rauch, I. Makkonen, On the formation of vacancy defects in III-nitride semiconductors, *J. Cryst. Growth* **350** (2012) 93
- [25] K. Köhler, R. Gutt, J. Wiegert, L. Kirste, Diffusion of Mg dopant in metal-organic vapor-phase epitaxy grown GaN and $\text{Al}_x\text{Ga}_{1-x}\text{N}$, *J. Appl. Phys.* **113** (2013) 073514
- [26] R. Jakiela, K. Gas, M. Sawicki, A. Barcz, Diffusion of Mn in gallium nitride: Experiment and modelling, *J. Alloys Comp.* **771** (2019) 215
- [27] F. Tuomisto, K. Saarinen, M. Bockowski, T. Suski, T. Paskova, and B. Monemar, Thermal stability of in-grown vacancy defects in GaN grown by hydride vapor phase epitaxy, *J. Appl. Phys.* **99** (2006) 066105
- [28] A. Uedono, Y. Tsukada, Y. Mikawa, T. Mochizuki, H. Fujisawa, H. Ikeda, K. Kurihara, K. Fujito, S. Terada, S. Ishibashi, S. F. Chichibu, Vacancies and electron trapping centers

in acidic ammonothermal GaN probed by a monoenergetic positron beam, *J. Crystal Growth* **448** (2016) 117

- [29] A. Uedono, M. Imanishi, M. Imade, M. Yoshimura, S. Ishibashi, M. Sumiya, Y. Mori, Vacancy-type defects in bulk GaN grown by the Na-flux method probed using positron annihilation, *J. Crystal Growth* **475** (2017) 261